Inhibition of explosive transitions in spreading dynamics by nonlinear higher-order adaptation

Longzhao Liu [1,2,3,4,5] Hongwei Zheng,[6] Zhihao Han [1,2] Xin Wang [1,2,3,4,5,7,*] and Shaoting Tang [1,8,2,9,3,4,5,†]

[1]*Institute of Artificial Intelligence, Beihang University, Beijing 100191, China*

[2]*Key laboratory of Mathematics, Informatics and Behavioral Semantics, Beihang University, Beijing 100191, China*

[3]*Zhongguancun Laboratory, Beijing 100094, China*

[4]*Beijing Advanced Innovation Center for Future Blockchain and Privacy Computing, Beihang University, Beijing 100191, China*

[5]*State Key Laboratory of Complex & Critical Software Environment, Beihang University, Beijing 100191, China*

[6]*Beijing Academy of Blockchain and Edge Computing, Beijing 100085, China*

[7]*State Key Laboratory of General Artificial Intelligence, BIGAI, Beijing 100080, China*

[8]*Hangzhou International Innovation Institute, Beihang University, Hangzhou 311115, China*

[9]*Institute of Medical Artificial Intelligence, Binzhou Medical University, Yantai 264003, China*

(Received 21 August 2025; accepted 1 July 2026; published 16 July 2026)

The coevolution of structure and dynamics, known as adaptation, is a fundamental property in various systems and drives diverse emergent behaviors. However, the adaptation in most works primarily stems from pairwise situations, which is insufficient to capture ubiquitous higher-order characteristics of real systems. Here, we introduce higher-order adaptation, characterized by baseline rewiring rate and nonlinear higher-order exponent, to model the coevolution of higher-order structure and spreading dynamics. We develop a hyperedge-based theoretical framework that well predicts critical behaviors and outbreak sizes. Notably, the inherent nonlinearity of higher-order adaptation inhibits bistability and explosive transitions, which is qualitatively opposite to the classical findings associated with pairwise adaptation or higher-order contagion. This inhibitory effect is enhanced by rewiring accuracy and remains robust across various adaptive spreading models. Our work establishes higher-order adaptation as a fundamentally distinct mechanism from pairwise adaptation, shedding light on adaptive systems.

DOI: 10.1103/5vff-syxb

I. INTRODUCTION

Complex systems, ranging from social to natural domains, can be typically modeled as networks and the dynamics on top of them, which jointly govern the emergent behaviors [1–4]. In particular, networks usually coevolve with the dynamics of nodes' states in real-world systems [5–7]. For instance, in the spreading of infectious diseases, healthy individuals may avoid contacts with infected ones, causing changes of network structure, which in turn affects the spreading dynamics. The mutual influence between structure and dynamics, known as adaptation, is identified as core mechanism in various systems and drives rich phenomena, such as bistability [8], echo chamber [9], and cooperation [10]. However, these works mainly concentrate on pairwise situations that assume all interactions between units are dyadic.

Recently, higher-order interactions among multiple units have been empirically observed across diverse systems and exhibit fundamental differences from pairwise interactions at multiple levels [11–15]. Structurally, such interactions require characterizations using higher-order structure such as hyperedges and simplicial complexes, which cannot be decomposed into pairwise links [16,17]. Dynamically, higher-order interactions are typically manifested as nonlinear dynamical mechanisms that lead to emergent behaviors beyond pairwise interactions [18–22]. For instance, higher-order spreading mechanism can induce the emergence of bistability and discontinuous transitions [23]. Higher-order games result in explosive transitions to cooperation [24]. In addition, recent studies provide frameworks of temporal higher-order networks and reveal their impacts on dynamical behaviors like percolation time and contagion thresholds [25–28]. Despite the progress, most works study higher-order network and dynamics separately, while real-world systems usually exhibit their coevolution, namely, higher-order adaptation. Take epidemic spreading as a paradigmatic example [29–31]. Individuals tend to leave groups with infection risks [8,32], and the likelihood of departure can nonlinearly increase with the group infection level. A recent study captures this nonlinear feature using a thresholdlike adaptation kernel and demonstrates its nonmonotonic effects on epidemic spreading [33]. COVID-19 pandemic also implies the nonlinear feature: Low-risk groups with few infections adopt minimal protective measures, whereas high-risk regions implement strict lockdown [34–36]. This reflects the evolution of higher-order structure induced by the number of infected individuals,

*Contact author: wangxin_1993@buaa.edu.cn

†Contact author: tangshaoting@buaa.edu.cn

Published by the American Physical Society under the terms of the Creative Commons Attribution 4.0 International license. Further distribution of this work must maintain attribution to the author(s) and the published article's title, journal citation, and DOI.

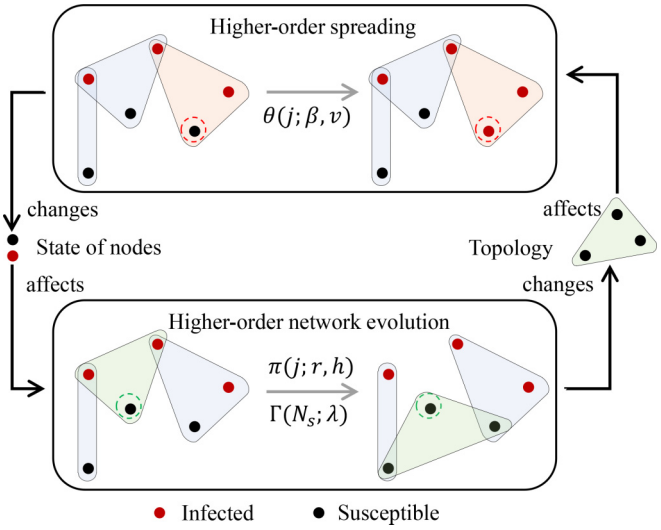

FIG. 1. Higher-order adaptive spreading model. It describes the coevolution of higher-order spreading and network topology. Specifically, the model incorporates higher-order adaptation characterized by a power-law kernel, to depict the evolution of higher-order network induced by higher-order spreading dynamics. In turn, network evolution alters the topological structure, which influences the outcomes of spreading dynamics occurring on top of it.

which in turn affects the epidemic spreading, forming a coevolutionary process. Nevertheless, it remains an open problem what fundamental rules of higher-order adaptation are and how they qualitatively affect dynamical behaviors.

Here, we propose adaptive spreading models with a higher-order adaptation kernel characterized by baseline rewiring rate and nonlinear higher-order exponent, and theoretically analyze the critical behaviors. Our results reveal rich and robust effects of higher-order adaptation. First, it can increase the thresholds. Second, compared to pairwise adaptation, nonlinear higher-order adaptation counterintuitively induces completely opposing emergent phenomena. The former enhances or induces bistability and explosive transitions, while the latter reduces or even eliminates them. Moreover, the inhibitory effect of nonlinear adaptation is more pronounced as rewiring accuracy increases. These findings, both theoretical and experimental, highlight the unique characteristics of higher-order adaptation in complex systems.

II. HIGHER-ORDER ADAPTIVE SPREADING MODEL

Our model is composed of two mutually interacting processes, including higher-order spreading and topological evolution, as shown in Fig. 1. First, we consider a typical spreading process on hypergraphs, where hyperedges of size m encode higher-order interactions among m individuals. Each node has two states: infected (I) and susceptible (S). Infected individuals recover at rate μ, while transmitting the disease to susceptible ones at a certain infection rate. Here, in line with higher-order spreading mechanisms in previous works [18,29,37], we adopt the nonlinear power-law infection rate

$$\theta(j;\beta,v) = \beta j^v, \tag{1}$$

where j is the number of infected nodes in the hyperedge, β is baseline infection rate, and v adjusts nonlinearity.

Next, we introduce higher-order adaptation to characterize how hypergraph evolves with the dynamical states of nodes. In real disease transmission, group-interaction environments with infected members, such as workplaces and schools, may take lockdown or closure measures as observed during the COVID-19 pandemic [34–36], and individuals tend to avoid contacts with infected persons [8,38]. These behaviors can be modeled as two decomposition mechanisms: (1) hyperedge breaking induced by closure measures and (2) removal of susceptible nodes from hyperedges due to individuals' risk-avoidance behaviors. Here, we focus on the hyperedge-breaking mechanism in the article and present the latter in Sec. VIII of the Supplemental Material [39]. Note that the likelihood of taking measures may nonlinearly rise as the number of infections increases [40,41]. Therefore, we assume that a hyperedge containing $j(j \geqslant 1)$ infected nodes and at least one susceptible node breaks with a power-law rate

$$\pi(j;r,h) = r j^h, \tag{2}$$

where r is baseline rewiring rate and h is nonlinear higher-order exponent. If $j = 0$, the hyperedge never breaks. $h = 0$ means that the breaking rate is independent of the number of infected nodes. $h > 0$ reflects more realistic higher-order property that does not appear in pairwise situations.

Moreover, to prevent network fragmentation and for the sake of analytical tractability, we assume that a new m-hyperedge will form when a m-hyperedge breaks. Specifically, a susceptible node of the broken hyperedge will choose $m-1$ nodes to form a new one. Inspired by the fitness in evolutionary game theory [42], we can define the probability that a susceptible node is chosen, which is

$$\Gamma(N_s;\lambda) = \frac{\lambda N_s}{\lambda N_s + (N - N_s)}, \tag{3}$$

where N and N_s represent the number of nodes and susceptible nodes, respectively. The parameter $\lambda \in [1,\infty)$ reflects the rewiring accuracy, which is influenced by the completeness and accuracy of information about the infection status of populations. Specifically, $\lambda = 1$ corresponds to random selection, while $\lambda \to \infty$ indicates perfect accuracy in selecting susceptible nodes.

III. RESULTS ON REAL HYPERGRAPHS

We use three human colocation datasets to derive hypergraphs [43,44,46], and then perform model simulations on top of them using Gillespie algorithm (see Sec. II of the Supplemental Material [39]). Figure 2 shows results on a real hypergraph, i.e., how epidemic prevalence varies against infection rate β under different parameters. Figure 2(a) reproduces the impacts of higher-order spreading mechanisms, such as inducing bistability and explosive transitions [23]. The former means coexistence of epidemic extinction and outbreak where the prevalence is determined by initial density of infected individuals, while the latter reveals the catastrophic growth of prevalence around thresholds. Both are qualitative phenomena that receive considerable attention. Here, our

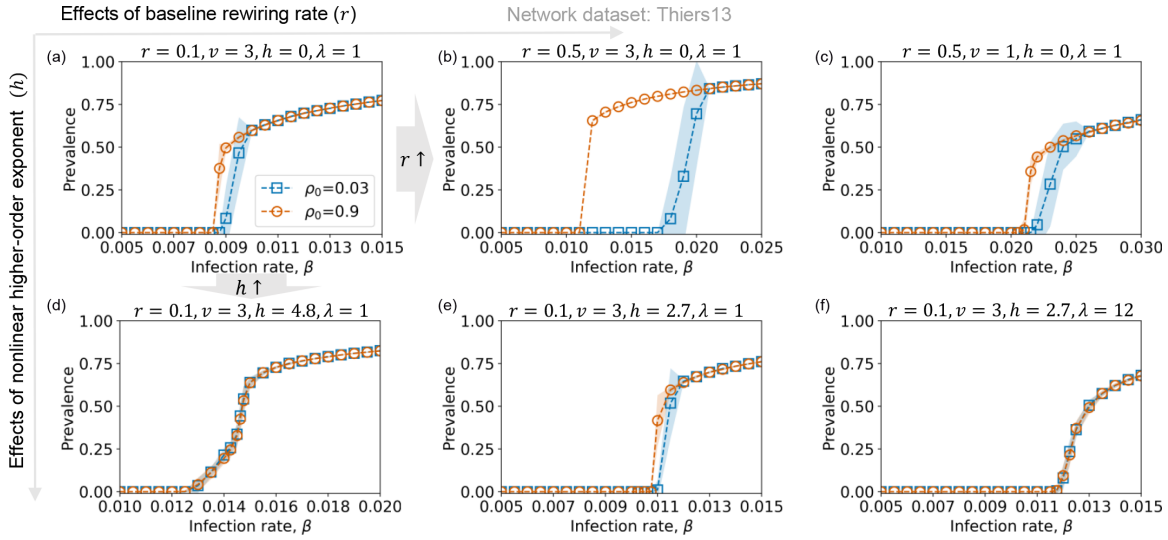

FIG. 2. Results based on a real hypergraph derived from Thiers13 dataset [43]. Shown is epidemic prevalence against infection rate β under different parameters. Each point is averaged over 30 runs, and the shaded area represents standard deviation. ρ_0 denotes the initial density of infected individuals. (a)–(c) Effects of baseline rewiring rate r. We present cases under different r and v, which show that larger r can amplify or induce bistability and explosive transitions. (d) Effects of nonlinear higher-order exponent h. Comparing panel (a) and (d), we highlight that increasing h alone can eliminate both the bistability and explosive transitions. (e), (f) Moreover, we present cases under different rewiring accuracy λ and show that a smaller value of h can eliminate these qualitative phenomena at higher λ. Other parameter: $\mu = 0.2$.

primary focus is to explore how adaptation mechanisms affect thresholds and these qualitative phenomena.

First, we explore the impacts of baseline rewiring rate r in the absence of nonlinear higher-order effects, i.e., $h = 0$. From Fig. 2(a) to Fig. 2(b), we show that a larger rewiring rate increases the thresholds and enlarges the bistable region. Furthermore, Fig. 2(c) presents the case where higher-order spreading mechanism is removed ($v = 1$). We find that bistability and explosive transitions can be induced solely by the baseline rewiring rate, which is similar to findings typically associated with pairwise adaptation [8]. Overall, the baseline rewiring rate not only provides an alternative pathway to explosive transitions and bistability, but also enhances these phenomena triggered by higher-order spreading.

Then, we focus on the nonlinear higher-order exponent h, which characterizes the inherent nonlinearity of higher-order adaptation. Figure 2(d), in comparison with Fig. 2(a), reveals its complex effects. Specifically, increasing h raises the critical thresholds. Notably, a larger nonlinear exponent leads to the disappearance of bistability and explosive transitions, which is qualitatively opposite to results obtained from the baseline rewiring rate and pairwise adaptation [8]. In addition, this nonlinearity-induced effect is enhanced at higher rewiring accuracy λ, where a smaller value of h is sufficient to eliminate bistability and explosive phenomena [see Figs. 2(e) and 2(f)]. The robustness of these findings is also verified on other real hypergraphs (see Fig. S1 of the Supplemental Material [39]).

IV. THEORETICAL FRAMEWORK AND RESULTS ON SYNTHETIC HYPERGRAPHS

What microscopic mechanism gives rise to the dramatically opposed dynamical behaviors we observe? In this section, we further develop a theoretical framework and explore cases on synthetic hypergraphs in order to get analytical insights and mechanistic explanations. We begin with the simplest m-uniform hypergraph, where all hyperedges contain m nodes and nodes' hyperdegrees follow a Poisson distribution. Despite the setup, it remains challenging to obtain a theoretical framework for higher-order adaptive dynamics due to the intricate correlations between structure and dynamics. Here, inspired by the ideas of pairwise approximation and generalized approximate master equations [8,33], we introduce hyperedge-based approximation framework to characterize the coevolutionary dynamics.

Let $N_i(t)$ denote the number of infected individuals at time t. $l_{m,k}(t)$ denotes the number of m-hyperedges containing k infected nodes. Then, the average rate, that an S node becomes infected, can be approximated by

$$\Theta = \sum_{j=1}^{m} \frac{(m-j)l_{m,j}}{N-N_i}\beta j^v, \tag{4}$$

where $(m-j)l_{m,j}/(N-N_i)$ represents the probability that the S node belongs to m-hyperedges containing j infected nodes. Thus, the dynamical equation for the number of infected nodes can be written as

$$\frac{dN_i}{dt} = -\mu N_i + (N-N_i)\Theta. \tag{5}$$

Equation (4) suggests that Θ depends on dynamic variables $l_{m,k}(t)$, $0 \leqslant k \leqslant m$. Thus, analyzing system behaviors also requires the dynamical equations of $l_{m,k}(t)$. Specifically, its evolution is composed of two parts: hyperedge rewiring as well as the change of nodes' state triggered by spreading

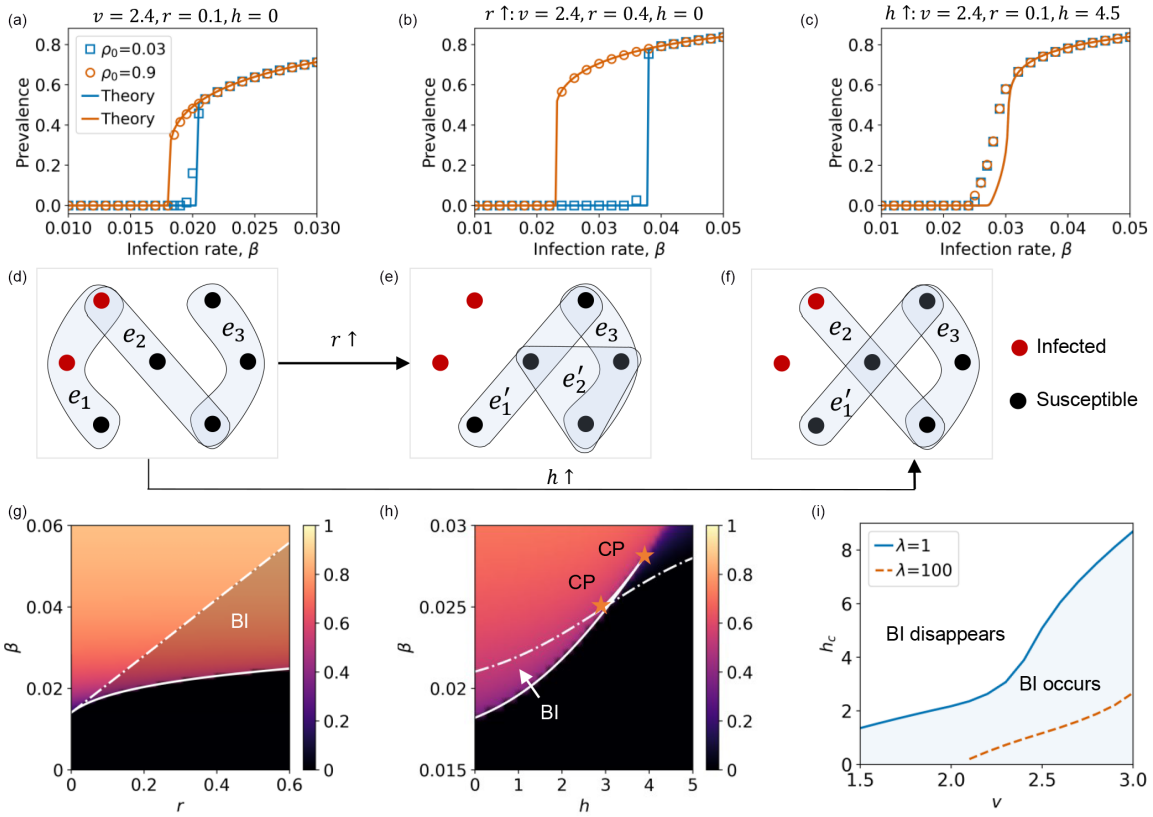

FIG. 3. Theoretical and simulation results on uniform hypergraphs. Epidemic prevalence is shown under different settings: (a) $r = 0.1$, $h = 0$; (b) $r = 0.4$, $h = 0$; and (c) $r = 0.1$, $h = 4.5$. In all cases, $\lambda = 1$. (d)–(f) Microscopic dynamical features of baseline rewiring rate r and nonlinear higher-order exponent h, which could intuitively explain their rich effects. Phase diagrams with different parameters: (g) $h = 0$, $\lambda = 1$; and (h) $r = 0.1$, $\lambda = 1$. The dashed line, representing the invasion threshold, is computed by Eq. (7) and the solid line, representing the persistence threshold, is numerically solved by Eqs. (5) and (6). The area they enclose is bistable region, abbreviated as BI. Moreover, there emerge cusp points in panel (h), which are derived through bifurcation analysis using MatCont [47]. We find that increasing r enlarges bistable region, whereas increasing h inhibits bistability and explosive transitions, both of which disappear once $h > h_c$. (i) The value of h_c under different parameters: $\lambda = 1$ (blue solid line) and $\lambda = 100$ (orange dashed line). Results show that h_c increases with v but decreases with λ. Other parameters: $N = 10000$, $E = 20000$, $v = 2.4$, $\mu = 0.2$.

processes. Consequently, we can obtain

$$\begin{aligned}\frac{dl_{m,k}}{dt} =& -(\beta k^v + \Theta)(m-k)l_{m,k} - \mu k l_{m,k} \\ &+ (\beta(k-1)^v + \Theta)(m-k+1)l_{m,k-1} \\ &+ \mu(k+1)l_{m,k+1} - r k^h l_{m,k} \\ &+ \sum_{j=1}^{m-1} l_{m,j} r j^h \binom{m-1}{k} \Gamma^{m-k-1}(1-\Gamma)^k, \\ \frac{dl_{m,m}}{dt} =& -\mu m l_{m,m} + (\beta(m-1)^v + \Theta) l_{m,m-1}, \end{aligned} \tag{6}$$

where Γ varies with N_i according to Eq. (3). The first equation depicts the cases $k = 1, 2, \ldots, m-1$. Its first four terms represent the changes caused by spreading dynamics, while the remaining terms describes hyperedge breaking and formation. Note that the total number of hyperedges, denoted by E, is constant, i.e., $\sum_{j=0}^{m} l_{m,j}(t) = E$. Thus, Eqs. (5) and (6) constitute a self-contained autonomous system with $m+1$ dimensions. When $m = 2$ and $\lambda = 1$, the equations would reduce to the classical model of adaptive pairwise networks [8].

Without loss of generality, we primarily concentrate on more intriguing yet still theoretically tractable higher-order cases, i.e., $m = 3$. In this situation, Eqs. (5) and (6) can be expressed as a four-dimensional system of differential equations. It has a trivial fixed point at the origin of coordinate system, and the stability condition of this point corresponds to the invasion threshold that determines whether epidemic outbreaks at small ρ_0. Here, we analyze its stability by linearizing the system and examining whether all eigenvalues of the Jacobian matrix have negative real parts (see Sec. IV of the Supplemental Material [39]). We then obtain the invasion threshold

$$\beta_c = \frac{\Omega + \sqrt{\Omega^2 + 2^{v+3}\langle d\rangle(\mu + r)(2\mu + 2^h r)}}{2^{v+2}\langle d\rangle}, \tag{7}$$

where

$$\Omega = 2^{h+1} r(1 - \langle d\rangle) - 4\mu\langle d\rangle.$$

Here, $\langle d\rangle = 3E/N$ represents the average hyperdegree. Note that the invasion threshold β_c is independent of rewiring accuracy λ.

As shown in Figs. 3(a)–3(c), our theoretical results agree well with simulations across various parameter settings.

Moreover, results on synthetic hypergraphs confirm that baseline rewiring rate amplifies bistability and explosive transitions induced by higher-order spreading, whereas nonlinear higher-order exponent eliminates these phenomena. We further provide intuitive explanations from microscopic aspects in Figs. 3(d)–3(f). Higher-order spreading mechanism, which is the main cause of bistability in Fig. 3(a), operates exclusively on hyperedges containing multiple infected nodes, such as e_1 in Fig. 3(d). The rise of baseline rewiring rate uniformly increases the breaking probability of hyperedges containing any infected nodes, which produces two key effects. The first one is to disrupt structural foundation of higher-order spreading, which inhibits bistability. The second one is to induce bistability due to the following reason: It triggers complete separation between S and I at small ρ_0 [see Fig. 3(e)], resulting in disease extinction, while at large ρ_0, complete separation is difficult to achieve, allowing the disease to persist. Notably, the second effect plays a dominant role. Furthermore, we explain why nonlinear higher-order exponent produces opposite impacts. It characterizes the nonlinear enhancement of hyperedge breaking rate with respect to the number of infected nodes. That means hyperedges containing two infected nodes possibly break, whereas those involving only one infected node remain intact, as shown in Fig. 3(f) (see Fig. S3 of the Supplemental Material [39] for quantitative descriptions). This not only disrupts the foundation of higher-order spreading but also preserves connections between S and I nodes. Both hinder the emergence of bistability and explosive phenomena.

To obtain more comprehensive insights, in Figs. 3(g) and 3(h) we plot phase diagrams for epidemic prevalence, with critical thresholds indicated by white lines. Figure 3(g) shows that the baseline rewiring rate increases the thresholds and the scope of bistable region. Figure 3(h) systematically reveals the diverse impacts of nonlinear higher-order exponent h. In addition to increasing critical thresholds, we observe the following qualitative changes. Specifically, as h increases, the bistable region gradually shrinks and eventually disappears. During the shrinkage, the nature of bistability shifts from coexistence of extinction and outbreak to coexistence of two outbreak states. Correspondingly, the system evolves from an explosive hybrid transition characterized by a discontinuous jump with critical scaling to a regime where continuous and hybrid transitions coexist, and finally to a continuous transition, with cusp points (CPs) separating the regimes (see Fig. S4 of the Supplemental Material [39]). Figure 3(i) further shows the critical value h_c at which bistability and explosive transitions disappear. We find that h_c increases with higher-order spreading parameter υ but decreases at higher rewiring accuracy λ. This indicates that λ enhances the inhibitory effect of h on explosive phenomena. In addition, when excluding the influence of higher-order spreading ($\upsilon = 1$), rewiring accuracy plays a pivotal role in eliminating explosive transitions caused by r (see Fig. S5 of the Supplemental Material [39]).

Furthermore, the qualitative effect of nonlinear higher-order exponent is robust across different settings, including $m = 4$, different system sizes, alternative rewiring schemes, and adaptive susceptible-infectious-recovered-susceptible (SIRS) spreading dynamics (see Secs. V and VII–IX of the Supplemental Material [39]). Crucially, the inhibitory effect of higher-order adaptation robustly holds for a general adaptation kernel beyond the power-law form (see Secs. X and XI of the Supplemental Material [39]).

V. CONCLUSIONS

This work introduces higher-order adaptation characterized by a power-law kernel to describe the widespread coevolution of higher-order networks and spreading dynamics in real systems. We provide a hyperedge-based theoretical framework whose predictions accurately capture the dynamical behaviors observed in agent-based simulations. Results on both synthetic and real hypergraphs reveal the counterintuitive impact of higher-order adaptation. Specifically, its inherent nonlinearity inhibits or even eliminates bistability and explosive transitions, which is qualitatively opposite to classical findings derived from pairwise adaptation or higher-order contagion. This inhibitory effect is strengthened with higher rewiring accuracy. Furthermore, similar inhibitory effect is also observed under different hyperedge sizes, rewiring mechanisms, higher-order spreading models, and adaptation kernels, demonstrating the robustness and generality of our main finding.

Our findings unveil complex impacts and unique dynamical properties of higher-order adaptation, transcending current understanding gleaned from pairwise adaptation. While this work focuses on coevolution of higher-order networks and spreading dynamics, the idea and framework of higher-order adaptation could be extended to study a broad class of adaptive systems, ranging from rumor contagion and opinion formation to evolutionary dynamics [48–50]. Besides, although the proposed higher-order adaptation is representative, there still exist many other higher-order adaptive mechanisms, which are worthy of further explorations, for instance, thresholdlike nonlinear relationship between structural evolution and the number of infected members, and flow of nodes among hyperedges of different scales [28,33].

ACKNOWLEDGMENTS

This work was supported by National Science and Technology Major Project (2022ZD0116800), Program of National Natural Science Foundation of China (12425114, 62141605, 12201026, 12301305, 62441617, 12501702), the Fundamental Research Funds for the Central Universities, Beijing Natural Science Foundation (Z230001), the Opening Project of the State Key Laboratory of General Artificial Intelligence (SKLAGI2025OP16), and Bejing Advanced Innovation Center for Future Blockchain and Privacy Computing.

DATA AVAILABILITY

The real hypergraph data that support the findings of this article are openly available [43–45].

[1] S. Boccaletti, V. Latora, Y. Moreno, M. Chavez, and D.-U. Hwang, Complex networks: Structure and dynamics, Phys. Rep. **424**, 175 (2006).

[2] S. N. Dorogovtsev, A. V. Goltsev, and J. F. F. Mendes, Critical phenomena in complex networks, Rev. Mod. Phys. **80**, 1275 (2008).

[3] A. Barrat, M. Barthelemy, and A. Vespignani, *Dynamical Processes on Complex Networks* (Cambridge University Press, Cambridge, UK, 2008).

[4] W. Zhu, X. Wang, C. Wang, L. Liu, H. Zheng, and S. Tang, Reputation-based synergy and discounting mechanism promotes cooperation, New J. Phys. **26**, 033046 (2024).

[5] R. Berner, T. Gross, C. Kuehn, J. Kurths, and S. Yanchuk, Adaptive dynamical networks, Phys. Rep. **1031**, 1 (2023).

[6] T. Gross and B. Blasius, Adaptive coevolutionary networks: A review, J. R. Soc. Interface **5**, 259 (2008).

[7] L. Liu, X. Wang, Y. Zheng, W. Fang, S. Tang, and Z. Zheng, Homogeneity trend on social networks changes evolutionary advantage in competitive information diffusion, New J. Phys. **22**, 013019 (2020).

[8] T. Gross, C. J. D. D'Lima, and B. Blasius, Epidemic dynamics on an adaptive network, Phys. Rev. Lett. **96**, 208701 (2006).

[9] X. Wang, A. D. Sirianni, S. Tang, Z. Zheng, and F. Fu, Public discourse and social network echo chambers driven by sociocognitive biases, Phys. Rev. X **10**, 041042 (2020).

[10] F. Fu, C. Hauert, M. A. Nowak, and L. Wang, Reputation-based partner choice promotes cooperation in social networks, Phys. Rev. E **78**, 026117 (2008).

[11] F. Battiston, G. Cencetti, I. Iacopini, V. Latora, M. Lucas, A. Patania, J.-G. Young, and G. Petri, Networks beyond pairwise interactions: Structure and dynamics, Phys. Rep. **874**, 1 (2020).

[12] A. Santoro, F. Battiston, G. Petri, and E. Amico, Higher-order organization of multivariate time series, Nat. Phys. **19**, 221 (2023).

[13] J. Grilli, G. Barabás, M. J. Michalska-Smith, and S. Allesina, Higher-order interactions stabilize dynamics in competitive network models, Nature (London) **548**, 210 (2017).

[14] G. Burgio, S. Gómez, and A. Arenas, Triadic approximation reveals the role of interaction overlap on the spread of complex contagions on higher-order networks, Phys. Rev. Lett. **132**, 077401 (2024).

[15] R. Lambiotte, M. Rosvall, and I. Scholtes, From networks to optimal higher-order models of complex systems, Nat. Phys. **15**, 313 (2019).

[16] D. Shi and G. Chen, Simplicial networks: A powerful tool for characterizing higher-order interactions, Natl. Sci. Rev. **9**, nwac038 (2022).

[17] S. Boccaletti, P. De Lellis, C. I. del Genio, K. Alfaro-Bittner, R. Criado, S. Jalan, and M. Romance, The structure and dynamics of networks with higher order interactions, Phys. Rep. **1018**, 1 (2023).

[18] G. Ferraz de Arruda, A. Aleta, and Y. Moreno, Contagion dynamics on higher-order networks, Nat. Rev. Phys. **6**, 468 (2024).

[19] F. Battiston, E. Amico, A. Barrat, G. Bianconi, G. Ferraz de Arruda, B. Franceschiello, I. Iacopini, S. Kéfi, V. Latora, Y. Moreno, *et al.*, The physics of higher-order interactions in complex systems, Nat. Phys. **17**, 1093 (2021).

[20] S. Majhi, M. Perc, and D. Ghosh, Dynamics on higher-order networks: A review, J. R. Soc. Interface **19**, 20220043 (2022).

[21] F. Malizia, S. Lamata-Otín, M. Frasca, V. Latora, and J. Gómez-Gardeñes, Hyperedge overlap drives explosive transitions in systems with higher-order interactions, Nat. Commun. **16**, 555 (2025).

[22] L. Neuhäuser, A. Mellor, and R. Lambiotte, Multibody interactions and nonlinear consensus dynamics on networked systems, Phys. Rev. E **101**, 032310 (2020).

[23] I. Iacopini, G. Petri, A. Barrat, and V. Latora, Simplicial models of social contagion, Nat. Commun. **10**, 2485 (2019).

[24] A. Civilini, O. Sadekar, F. Battiston, J. Gómez-Gardeñes, and V. Latora, Explosive cooperation in social dilemmas on higher-order networks, Phys. Rev. Lett. **132**, 167401 (2024).

[25] L. Di Gaetano, F. Battiston, and M. Starnini, Percolation and topological properties of temporal higher-order networks, Phys. Rev. Lett. **132**, 037401 (2024).

[26] G. Petri and A. Barrat, Simplicial activity driven model, Phys. Rev. Lett. **121**, 228301 (2018).

[27] Z. Han, L. Liu, X. Wang, Y. Hao, H. Zheng, S. Tang, and Z. Zheng, Probabilistic activity driven model of temporal simplicial networks and its application on higher-order dynamics, Chaos **34**, 023137 (2024).

[28] I. Iacopini, M. Karsai, and A. Barrat, The temporal dynamics of group interactions in higher-order social networks, Nat. Commun. **15**, 7391 (2024).

[29] G. St-Onge, H. Sun, A. Allard, L. Hébert-Dufresne, and G. Bianconi, Universal nonlinear infection kernel from heterogeneous exposure on higher-order networks, Phys. Rev. Lett. **127**, 158301 (2021).

[30] W. Wang, Y. Nie, W. Li, T. Lin, M.-S. Shang, S. Su, Y. Tang, Y.-C. Zhang, and G.-Q. Sun, Epidemic spreading on higher-order networks, Phys. Rep. **1056**, 1 (2024).

[31] Y. Chen, Y. R. Gel, M. V. Marathe, and H. V. Poor, A simplicial epidemic model for covid-19 spread analysis, Proc. Natl. Acad. Sci. USA **121**, e2313171120 (2024).

[32] V. Marceau, P.-A. Noël, L. Hébert-Dufresne, A. Allard, and L. J. Dubé, Adaptive networks: Coevolution of disease and topology, Phys. Rev. E **82**, 036116 (2010).

[33] G. Burgio, G. St-Onge, and L. Hébert-Dufresne, Characteristic scales and adaptation in higher-order contagions, Nat. Commun. **16**, 4589 (2025).

[34] S. Lai, N. W. Ruktanonchai, L. Zhou, O. Prosper, W. Luo, J. R. Floyd, A. Wesolowski, M. Santillana, C. Zhang, X. Du, *et al.*, Effect of non-pharmaceutical interventions to contain covid-19 in China, Nature (London) **585**, 410 (2020).

[35] N. Perra, Non-pharmaceutical interventions during the covid-19 pandemic: A review, Phys. Rep. **913**, 1 (2021).

[36] S. Flaxman, S. Mishra, A. Gandy, H. J. T. Unwin, T. A. Mellan, H. Coupland, C. Whittaker, H. Zhu, T. Berah, J. W. Eaton, *et al.*, Estimating the effects of non-pharmaceutical interventions on covid-19 in Europe, Nature (London) **584**, 257 (2020).

[37] G. St-Onge, I. Iacopini, V. Latora, A. Barrat, G. Petri, A. Allard, and L. Hébert-Dufresne, Influential groups for seeding and sustaining nonlinear contagion in heterogeneous hypergraphs, Commun. Phys. **5**, 25 (2022).

[38] R. Pastor-Satorras, C. Castellano, P. Van Mieghem, and A. Vespignani, Epidemic processes in complex networks, Rev. Mod. Phys. **87**, 925 (2015).

[39] See Supplemental Material at http://link.aps.org/supplemental/10.1103/5vff-syxb for details about data processing and model simulations, procedures of theoretical analysis, and results

under different hyperedge sizes, rewiring mechanisms, higher-order spreading models, and adaptation kernels for verifying robustness and generality of our findings, which includes Refs. [8,23,43,44,46,47].

[40] B. Morsky, F. Magpantay, T. Day, and E. Akçay, The impact of threshold decision mechanisms of collective behavior on disease spread, Proc. Natl. Acad. Sci. USA **120**, e2221479120 (2023).

[41] World Health Organization, Report of the WHO-China joint mission on coronavirus disease 2019 (COVID-19), 2020, https://www.who.int/docs/default-source/coronaviruse/who-china-joint-mission-on-covid-19-final-report.pdf.

[42] M. A. Nowak, *Evolutionary Dynamics: Exploring the Equations of Life* (Harvard University Press, Cambridge, MA, 2006).

[43] R. Mastrandrea, J. Fournet, and A. Barrat, Contact patterns in a high school: A comparison between data collected using wearable sensors, contact diaries and friendship surveys, PLoS One **10**, e0136497 (2015).

[44] M. Génois and A. Barrat, Can co-location be used as a proxy for face-to-face contacts? EPJ Data Sci. **7**, 11 (2018).

[45] http://www.sociopatterns.org.

[46] J.-G. Young, G. Petri, F. Vaccarino, and A. Patania, Construction of and efficient sampling from the simplicial configuration model, Phys. Rev. E **96**, 032312 (2017).

[47] A. Dhooge, W. Govaerts, Y. A. Kuznetsov, H. G. E. Meijer, and B. Sautois, New features of the software MatCont for bifurcation analysis of dynamical systems, Math. Comput. Modell. Dyn. Syst. **14**, 147 (2008).

[48] L. Liu, X. Wang, X. Chen, S. Tang, and Z. Zheng, Modeling confirmation bias and peer pressure in opinion dynamics, Front. Phys. **9**, 649852 (2021).

[49] N. E. Friedkin, A. V. Proskurnikov, R. Tempo, and S. E. Parsegov, Network science on belief system dynamics under logic constraints, Science **354**, 321 (2016).

[50] U. Alvarez-Rodriguez, F. Battiston, G. F. de Arruda, Y. Moreno, M. Perc, and V. Latora, Evolutionary dynamics of higher-order interactions in social networks, Nat. Hum. Behav. **5**, 586 (2021).